Morphology control of carbon nanotubes in continuously spun fibres

Rajyashree M. Sundaram*, Krzysztof K. K. Koziol and Alan H. Windle
Department of Materials Science and Metallurgy, University of Cambridge
Pembroke street, Cambridge, CB2 3QZ
*Corresponding author: rm533@cam.ac.uk

ABSTRACT

A novel chemical vapour deposition (CVD)-based approach resulting in the large-scale continuous production of macroscopic-assemblies (fibres/films) of pristine carbon nanotubes (CNTs), composed of principally single or double or multi-walled CNTs, with well-defined structural characteristics is reported. The synthesis has been further fine-tuned to directly produce metallic single-walled nanotube fibres, with a significant (near) armchair-CNT content. In this context, the duplex role of sulphur as a promoter and as a tool for catalyst-size control, in addition to the influence of orchestrated carbon, catalyst and sulphur-precursor pyrolysis, towards obtaining fibres comprising CNTs of selective morphologies and the resulting consequences on the fibre properties will be discussed

Keywords: Carbon nanotubes, chemical vapour deposition, morphology selective synthesis.

1 INTRODUCTION

Multifunctional attributes of carbon nanotubes (CNTs) have attracted the focus of industrial and academic communities alike. Translating the properties of individual CNTs into their macroscopic ensembles – fibres, yarns or films - is envisaged to uncover a vista of applications. The performance of the macroscopic assemblies relies on their internal structures which are in turn governed by the structural characteristics of the nanotubes i.e the number of walls, aspect ratio and chirality distributions. Ideally, materials of (near) homogeneous composition are preferred. While CNT production by chemical vapour deposition (CVD) is advantageous with its potential of scalability, the products are, in general, heterogeneous, requiring post-production purification and sorting. Reports on the CVD synthesis of CNTs of selective diameter distributions and controlled number of walls have often have drawn correlation between catalyst size and the diameter[1], type and morphology[2] of the nanotubes. In CVD reactions involving mobile catalyst particles in a gas flow (i.e floating catalyst processes), the key aspects that direct the catalyst dimensions include a) the mode of introduction of the catalyst - say in the form of colloids[3] or as molecular precursors[3a] which on thermolysis yield catalyst nanoparticles hence fixing the initial catalyst size distribution b) the growth dynamics of these catalyst clusters which is dependent on factors affecting collision probabilities – such as dilution and temperature[4].

We present a twist to our previously reported CVD-based continuous fibre production methodlgy[5], to obtain pristine macroscopic-assemblies (with >90% nanotube content), composed of principally single or double or multi-walled (SW, DW, MW) CNTs. The basic process involves the pyrolysis of a catalyst precursor (ferrocene) resulting in the in-situ production of catalyst (iron) nanoparticles, which grow and nucleate CNTs, with carbon supplied by the 'cracking' of a carbon source (hydrocarbons, alcohols etc.) in a hydrogen atmosphere. In addition, a sulphur precursor is incorporated to the reaction feedstock. The adding of sulphur, a recognised promoter in CNT growth, results in the production of exceptionally long CNTs (typically millimetres in length) that associate to form a nanotube plume with mechanical integrity which can be continuously spun into a fibre. In contrast to previously reported injection systems which have entailed injection of mixture of precursors in solution form[5,6], here we report the injection of all the feedstock components in a gaseous state which enables more uniform input of the compounds, in addition to providing flexibility to both the choice of compounds that can be used (irrespecitve of their mutual solubilities) and the parameter space that can be explored to achieve spinning. Using the gaseous-injection system, in the present report, we demostrate the effect of controlling the iron catalyst growth (orginating from thermal decomposition of ferrocene) and the effect of using sulphur precursors with varying thermal degradation behaviours on the morphology of the nanotubes in the fibres produced.

2 METHODS

The continuous spinning of CNT fibres (schematic as shown in Fig. 1a) was carried out in a vertical ceramic reactor (d=100 mm, L= 1800 mm). The gaseous feedstock consisting of methane (carbon precursor), sublimed ferrocene and sulphur-precursor vapours (originating from custom-made vapourisers, carried by helium), was introduced in to the reactor through a steel injector tube (d = 13 mm). The various sulphur precursors used were: Thiophene, carbon-di-sulphide (CDS), Hydrogen sulphide and sulphur vapour. The feedstock components carried by hydrogen travelled along the temperature profile of the reactor (Fig 1b) and thermolysed to produce a plume composed of entangled nanotubes that was continuously drawn at ~20 m min^{-1} and densified online with an acetone spray into a fibre (typically d=10 µ). The molar input rates of methane and hydrogen were obtained directly from the mass-flow controllers which regulated the input of these gases into the reactor. The molar input rates of ferrocene and the sulphur precursors have been obtained by
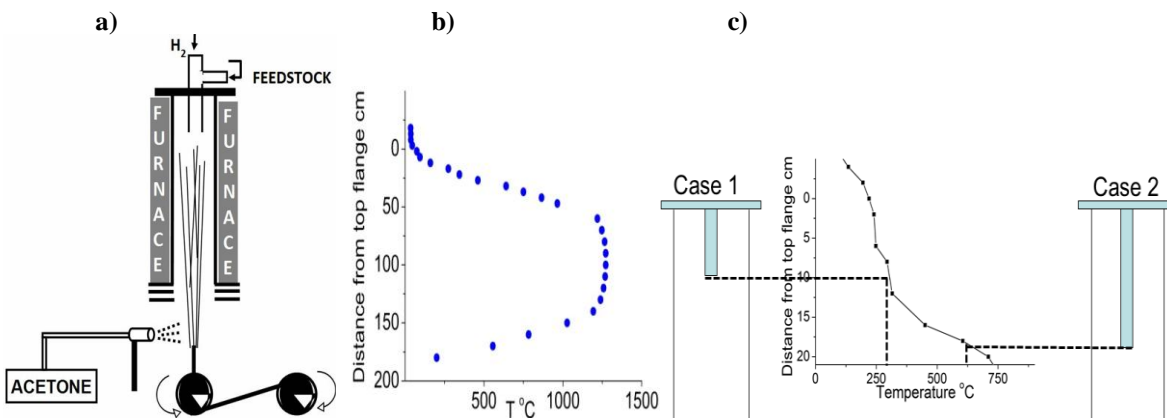
Fig 1 *a) The continuous fibre spinning set-up b) The temperature profie of the reactor c)The temperature profile of the top-zone and the two set-ups using different injector lengths*

calibrating the custom-made vapourisers (carried out gravimetric methods). The optimum molar input rates of the feedstock componenets to achieve continuous spinning with the various sulphur precursors are listed in Table 1.

The temperature of the feedstock mixture at the end of the main inlet, 100 mm of which was inserted in to the reactor was usually maintained under $400^{o}C$ (typically between 250-$350^{o}C$) as shown in Fig 1c (case 1). This ensured that the pyrolysis of the feedstock components specifically, ferrocene (which begins to thermolyse at~ $400^{o}C^{7}$), was initiated inside the reactor tube and not within the injector tube itself. In addition, as a special case, while injecting methane/ferrocene/thiophene feedstock (at identitical input rates of the individual precursors as in case 1), the temperature of the injector-end was increased to 600-$800^{o}C$ by extending the length of the main-inlet in to the furnace to ~180-200 mm (case 2, Fig 1c) to bring about the decomposition of ferrocene within the injector tube. This was done with the aim of altering the catalyst growth dyamics and to assess any changes in the nanotube-morphology constituting the product.

	Sulphur input (mol min^{-1}) (/10^{-5})	S/Fe		
		Optimum	**Range**	
CDS	36	170	114	219
S (g)	14	70	52	76
H$_2$S	15	95	86	130
C$_4$H$_4$S	3-5	15	10	30

Table 1: *The optaimal molar input rates of the various sulphur precursors injected in combination with methane (1.8 x 10^{-3} mol min^{-1}), ferrocene (1.8 – 2.1 x 10^{-6} mol min^{-1}) and hydrogen (4-7x10^{-2} mol min^{-1}).*

The analyses of the fibre microstructure were carried out by electron microscopy and Raman Spectroscopy (incident light of λ=633 and 514 nm). The fibres obtained were also subjected to thermogravimeteric analysis. Samples (~4mg) were heated to $1000^{o}C$ at a rate of $5^{o}C$ min^{-1} under air flow (60mL min^{-1}).The mechanical properties of the fibres were investigated with tensile tests using a dedicated fibre testing equipment. Testing was carried out at a standard gauge length of 20 mm and a test-speed of 2 mm min^{-1} to acquire the specific strength and specific stiffness (expressed in N Tex^{-1}, numerically equivalent to GPa

SG^{-1}, where Tex is g Km^{-1} and SG is specific gravity). The electrical conductivity values were obtained as $\sigma = R_{\Omega}$ (Resistance) X A_m^2 (cross-sectional area)/ L_m (fibre length) with 2-point measurements on ~ 5 cm segments of fibres using silver paint to establish contact. The cross-section, assumed as circular, was determined from the diameters measured in an optical microscope. In addition to expressing the conductivity values in conventional units of S m^{-1}, to eliminate inconsistencies arising from using cross-sectional areas (the diameter of the fibres vary along the length of the fibre significantly and the cross-section is not entirely circular) and since for applications density normalized values carry more sanctity, the specific conductivity values σ_{sp} (S cm^2 g^{-1})= Conductivity σ / volumetric density, calculated as [L_m X 10^7]/[R_{Ω} X $T_{g\ Km}^{-1}$] will also be furnished.

3   RESULTS AND DISCUSSION

The typical internal structures of the fibres produced using thiophene, CDS and Sulphur vapours as sulphur precursors, indicates (Fig 2a) minimal presence of extraneous materials at optimal feedstock injection conditions. This is in tune with the TGA results which shows catalyst residues as low as 2% and extraneous carbon content of 4-6% (measured as weight loss at $450^{o}C$, since the extraneous carbon contents being more defective combust at much lower tempartures than the nanotubes) signifying carbon nanotube content in the fibres ranging to >90%. The TEM analysis reveals distinctive differences in the diameters (Table 2) and number of walls (Fig 2b-d) of the nanotubes constituting the fibres. Fibres obtained in syntheses using thiophene as the sulphur precursor (Fig 2c) seemed to consist mainly of 5-10 nm collapsed DWCNTs (as in the previously reports[6]), while the syntheses employing CDS and sulphur vapour as the sulphur precursors seemed to yield SWCNT fibres (an illustrative example of bundles in fibres obtained with sulphur vapour as promoter precursor is shown in Fig 2b). However, production with methane/ferrocene/thiophene feedstock injected at higher injector-end temperature (Case 2 – Fig 1c) mainly seemed to yield MWCNT fibres (Fig 2d). The variation in the combustion temperatures (obtained from TGA) i.e 520, 580 and $620^{o}C$ for the SWCNT, DWCNT and MWCNT fibres respectively, is further proof to the nature of nanotubes (lower the number of walls, lower is the combustion temperature). Considering the I_D/I_G ratios, values for the SWCNT fibres obtained from CDS

and sulphur vapours are exceptionally low (~0.01-0.02) indicating minimal presence of impurities (in resonance with SEM and TGA results) along with high crystallinity of nanotubes. However, the DWCNT and MWCNT fibres (despite the identical levels of purity) showed higher I_D/I_G ratios (0.08 for DWCNT fibres and ~0.2 for MWCNT fibres), pointing to higher incidence of defects in the nanotubes themselves (which can perhaps be expected with the increase in the number of walls). At this juncture it is apt to mention that continuous spinning with H_2S was found to be difficult (and sufficient quantities could not collected to enable bulk TGA analysis or performance evaluation). However, the nanotubes in the discontinuously spun fibres were primarily found to be SWCNTs. The SEM analysis of these fibres revealed a product fraught with impurities, which was confirmed by the high I_D/I_G ratio of 0.8-1.0 obtained by Raman analysis.

To confirm the morphology of the fibres obtained, an in-depth analysis of the Raman spectra was carried out. The fibres obtained from syntheses employing H_2S, CDS and sulphur vapour, showed distinctive SWCNT features including the low frequency radial breathing modes (RBMs) shown in Fig 3a, G band with internal structure (G+ and G-) with the G+band occuring at ~1590 cm^{-1} (Fig 3 c), and a D band occuring at ~1320 cm^{-1}. In contrast, the DWCNT and MWCNT fibres showed typical absence of the RBMs (Fig 3a) and more graphite like G and D features; with the G peak occuring as a single Lorentzian peak at ~1580 cm^{-1} (Fig 3b) and the D peak at 1330 cm^{-1}. The diameters obtained by RBM analysis (in conjunction with the TEM diameter distribution) indicated the presence of bothe metallic and semiconducting SWCNTs in the case of fibres obtained from syntheses using H_2S and S (g). This is re-confirmed with the Lorentzian lineshape of the G- band, at 1573 cm^{-1}. The fibres obtained using CDS as the sulphur precursor (as reported elsewhere[8]), seem to be composed of mainly metallic nanotubes (any RBM resonances from non-metallic nanotubes were found absent and the G- band exhibited the Fano line shape with the peak position considerably downshifted to 1555 cm^{-1}) . More interestingly, most of these nanotubes also have been found to be armchair structures[8] as revealed by the spotty electron diffraction patterns in constrast to the continuos rings usually encountered for the other SW, DW and MWCNT fibres.

To explain the morphology control, it is essential to trace the growth and association of catalyst particles with sulphur (sulphudisation) that becomes available from the various S-precursors, from the point of their birth at 400^oC (by the decomposition of ferrocene), as they travel along the temperature profile of the reactor, until the point of nanotube nucleation and growth (at $T>1000^oC$, to add: carbon availability from methane – an exceptionally stable hydrocarbon – in the hydrogen atmosphere perhaps occurs around these temperatures[9]). Thiophene due to its aromaticity is much more stable and is expected to undergo dehydrosulphudisation at higher temperatures when sulphur (probably, in the form of H_2S) becomes available to interact with the iron catalyst particles, when they would have grown to larger sizes. However, in the case of using Sulphur vapour and CDS, sulphudisation is expected to take place at lower temperatures, when the catalyst sizes are small. Sulphur becomes available, by hydrogenation and the subsequent scission of C-S[10] bonds, in the case of CDS and in the case of sulphur vapour – the sulphudisation can be

expected to take place by direct combination or through a H_2S intermediate.
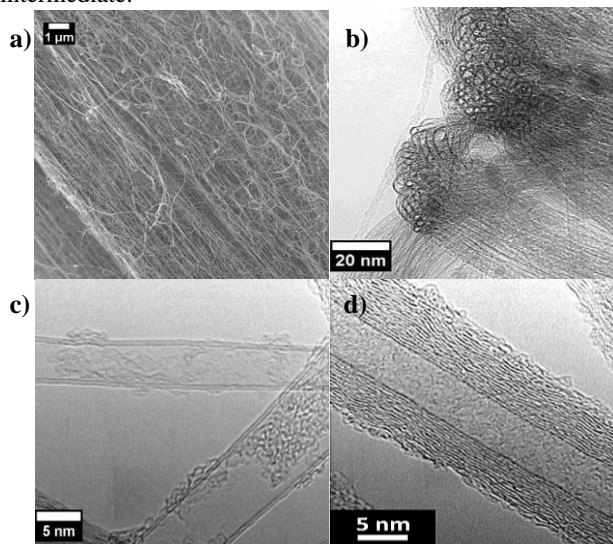
Fig 2 a) SEM image of a fibre spun at optimum injection conditions. Nanotubes in b) SWCNT c) DWCNT and d) MWCNT fibres.

It is assumed that sulphudisation preserves catalyst sizes. Indeed, literature on the production of carbon fibres, which frequently report the use sulphur compound additives to enhance graphitisation quality and yields, is supportive of this hypothesis[11]. Hence, while with thiophene DWCNT fibres are obtained, by employing early sulphudisation – with CDS and sulphur vapour as S-precursors, SWCNT fibres are obtained. Since, early sulphudisation takes place on a higher number of catalyst particles, which are smaller – and hence, with a higher fraction of surface atoms, the amount of sulphur-precurosr input required to sufficiently sulphudise the catalyst may be expected to be higher than what is required for late-sulphudisation (as can be seen from Table 1). It is also apt to recall at this juncture that although H_2S, when used directly as the S-precursor produces SWCNT fibres, the spinning has been observed to be discontinuous. This may be attributed to the poisoning of a majority of the catalyst particles, which are rendered inactive (contributing to the impurity content, along with self-pyrolysis methane occuring in the absence of catalyst adding carbonaceous impurities to the product). Hence, only a small fraction of the particles which happened to be optimally sulphudised are available leading to nanotube formation and fibre production.

For the production of MWCNT fibres from methane/ferronce/thiophene feedstock, a special combination of enhanced sintering and late sulphudisation (with thiophene) is required. The enhanced sintering is induced by forcing the initial catalyst cluster nucleation and growth to take place in the spatially constrained environment of the injector tube of d~13 mm instead of the reactor tube of d=100mm (case 2 Fig 1c). Hence, with the mean free path of the particles considerably reduced, despite the identical the input concentration of ferrocene and that of all other feedstock components, the mean size of the catalyst nanoparticles that participate in nucleation and growth of nanotubes is shifted to larger values, leading to the production of predominantly MWCNT fibres.
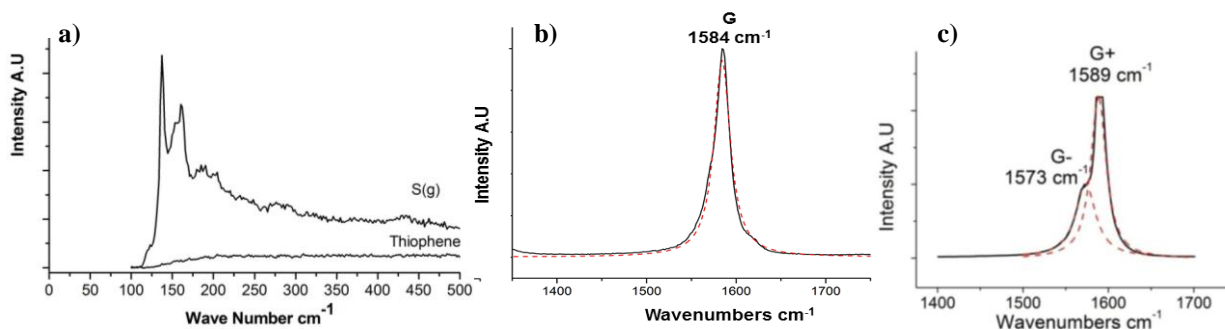
Fig 3 *a) RBM region of SWCNT and DW/MWCNT fibres b)G band of DW/MWCNT fibres c) G band of SWCNT fibres synthesised using sulphur vapour or H_2S along with methane and ferrocene.*

	TEM d_{CNT} (nm)
SWCNTs-CDS	1.4±0.3
SWCNTs – S (g)	1.7±0.4
SWCNTs – H_2S	2.4±1.0
DWCNTs	7.6±2.3
MWCNTs	20.5±7.7

Table 2 *Diameter of CNTs in the various fibres*

	Sp. strength GPa SG^{-1} (N Tex^{-1})	Sp. Stiffness GPa SG^{-1} (N Tex^{-1})	σ S m^{-1} (/ 10^5)	σ_{sp} S cm^2 g^{-1} (/10^4)
SWCNT – CDS	0.2±0.2	15.5±8.2	8.9 ± 1.5	1.8± 0.19
SWCNT – S (g)	0.3±0.1	12.8±7.5	5.5 ± 1.0	1.2± 0.15
DWCNT	0.9±0.1	42.2±10.1	0.7± 0.2	0.8± 0.2
MWCNT	0.3 ± 0.1	18.6 ± 6.0	0.2±0.08	0.3± 0.1

Table 3 *Properties of the SW, DW and MWCNT fibres*

Now, considering the properties of the various fibres: the morphology of the nanotubes can be noticed to distinctily affect the performance (Table 3). The specific strength and stiffness of the SWCNT fibres are typically lower than the DWCNT counterparts. This can be expected, as the shared contact area between the nanotubes within the bundles is likely to be smaller in the case of SWCNT fibres than in the DWCNT fibres. However, the SWCNT fibres have higher conductivity values than the DWCNT and MWCNT fibres, perhaps attributable to the lower incidence of intrinsic defects in the nanotubes; with the metallic nanotube fibres (synthesised with CDS as the sulphur precursor) predictably showing the highest conductivity values. The poor performance of the MWCNT fibres is due to the poorer bundling capability and possibly higher intrinsic defect density of the nanotubes in the fibres.

4 CONCLUSIONS

We reveal the duplex role of sulphur-precursors, which while acting as the oft-reported promoter generators, can also function as tools for catalyst-size control – hence, dictating the nanotube diameter and type. We examined the effects of orchestrated thermal degradation of ferrocene and various sulphur-precursors (carbon-disulphide, hydrogen sulphide, sulphur vapour and thiophene) with diverse thermolysis and sulphudisation behaviours on the growth dynamics of the catalyst, which by default, grows by collision, under a positive temperature gradient in the reactor tube in the continuous spinning process . The result was evidenced in the distinct differences in the diameter and number of walls of the nanotubes in the fibre product. Furthermore, the CNT morphology was found to have an influence, as may be expected, on the properties of the fibres, at identical product-purity levels.

REFERENCES

[1] Nasibulin, A. G., P. V. Pikhitsa, H. Jiang, E. I. Kauppinen , Carbon, 43(11), 2251-2257, 2005.
[2] Schäffel. F, Rümmeli M. H, Kramberger C, Queitsch U, Mohn E, Kaltofen R, Pichler T, Büchner B, Rellinghaus B and Schultz L, Phys. Status Solidi A, 205, 1382–1385, 2008
[3] Takeshi Saito,Satoshi Ohshima,Wei-Chun Xu, Hiroki Ago, Motoo Yumura and Sumio Iijima, The Journal of Physical Chemistry B 109 (21), 10647-10652, 2005; [3a] A Moisala, A. G. Nasibulin, D. P. Brown, H. Jiang, L. Khriachtchev, E. I. Kauppinen, Chemical Engineering Science 61 (2006) 4393 – 4402
[4] D. Conroy, A Moisala, S Cardoso, A Windle, J Davidson Chemical Engineering Science, 65(10), 2965-2977, 2010; A. Barreiro, C. Kramberger, M.H. Rümmeli, A. Grüneis, D. Grimm, S. Hampel, T. Gemming, B. Büchner, A. Bachtold, T. Pichler, Carbon, 45(1), 55-61, 2007
[5] Ya-Li Li,Ian A. Kinloch, and Alan H. Windle Science 304 (5668), 276-278, 2004
[6] Krzysztof Koziol, Juan Vilatela, Anna Moisala, Marcelo Motta, Philip Cunniff, Michael Sennett, and Alan Windle Science 318 (5858), 1892-1895, 2007.
[7] Kazunori Kuwana, Kozo Saito Proceedings of the Combustion Institute, 31, 1857–1864, 2007
[8] Sundaram, R. M., Koziol, K. K. K. and Windle, A. H. Adv. Mater., 23, 5064–5068, 2011
[9] Christophe Guéret, Michel Daroux, Francis Billaud, Chemical Engineering Science, 52 (5), 815-827, 1997
[10] X. Devaux, S.Yu. Tsareva, A.N. Kovalenko, K.S. Zaramenskih, E. McRae, E.V. Zharikov, Physica E: Low-dimensional Systems and Nanostructures, Available online http://dx.doi.org/10.1016/j.physe.2010.11.014, 2010
[11] Yue-Ying Fan, Hui-Ming Cheng, Yong-Liang Wei, Ge Su, Zu-Hong Shen, Carbon, 38 (6), 921-927, 2000